Thermal Field-Flow Fractionation of Polymers with Exponential Temperature Programming†

J. J. Kirkland* and W. W. Yau

E. I. du Pont de Nemours and Company, Central Research and Development Department, Experimental Station, Wilmington, Delaware 19898. *Received January 14, 1985*

ABSTRACT: Broad molecular weight distributions of a wide range of organic-soluble macromolecules are best characterized with thermal field-flow fractionation (TFFF) by programming a temperature-gradient (ΔT) decrease during separation so that increasing molecular weights successively elute in a reasonable time. TFFF separations are achieved by applying a relatively large thermal gradient across a single flowing mobile phase in a thin channel. The method demonstrates about 5-fold greater resolution than high-performance size-exclusion chromatography (SEC), and fragile polymers of very high molecular weight (>10^7 MW) can be analyzed. A convenient TFFF programming technique involves maintaining a constant ΔT for a time τ after sample injection and then exponentially decreasing ΔT also with the time constant τ. In this time-delay exponential force field-decay TFFF method (TDE-TFFF), a plot of log MW vs. retention is a linear relationship that provides an accurate calibration for molecular weight distribution (MWD) measurements over a wide MW range. Broad MWD polystyrene and poly(methyl methacrylate) samples have been characterized by this method.

Introduction

A relatively new family of separation methods called field-flow fractionation (FFF) permits the characterization of a wide variety of particulates and soluble macromolecules in the broad molecular weight range of about 10^3–10^{16}, corresponding to particle diameters from about 10^{-3} to 10^2 μm.[1-4] FFF is comparable in separation power to other high-resolution methods such as gas and liquid chromatography; however, applications generally are in areas in which these methods do not apply.

FFF, sometimes described as one-phase chromatography, is performed in a thin, open channel. Since there is no separate stationary phase used in FFF, solute retention results from the redistribution from fast- to slow-moving streams of the laminar flow profile generated within the flowing liquid mobile phase. Upon injection, sample components are evenly distributed across a narrow rectangular channel. Application of an applied external force field perpendicular to the channel causes sample components to crowd against one wall. Solvent and other low molecular weight components are unaffected by the force field, and, therefore, move downstream in the channel at the average velocity of the laminar flow stream. In contrast, larger sample components that are crowded close to the wall by the external force field are carried downstream only by slower-moving streams near the wall so that they lag behind and elute after the solvent.

Previous work in this laboratory involved the development of sedimentation FFF (SFFF), where the external force field is centrifugal.[3,4] SFFF equipment has been developed that allows force fields up to 100 000 gravities (at 32 000 rpm rotor speed), which permits the characterization of a wide range of particulates and soluble macromolecules largely in aqueous mobile phases.

Thermal FFF (TFFF) is a high-resolution separation method for relatively nonpolar polymers in appropriate organic solvents.[5-8] The TFFF technique is thought to be based on the principle of thermal diffusion. However, since the mechanism of this effect is not well understood, the dependence of polymer type difference on retention for the TFFF method is not yet predictable. For example, water-soluble species apparently respond weakly to the external thermal gradient and display little of the thermal diffusion process. Efforts to retain such materials in purely aqueous mobile phases thus far have not been successful.[7]

† Presented in part at the fall meeting of the American Chemical Society, Aug 27–31, 1984, Philadelphia, PA.

The object of this study was to develop the equipment and techniques to permit quantitative measurements of molecular weight distribution on a variety of organic-soluble macromolecules. Specific importance was placed on developing temperature programming techniques to permit the accurate analysis of polymers with broad molecular weight distributions.

Theory

With the TFFF method a temperature gradient is established betwen two parallel, highly polished conductive metal bars, and a channel is formed by an insulating spacer. Solutes are transported by thermal diffusion, presumably toward the cold wall.[9] Typical of all FFF methods, separation results from solutes being forced to different average distances from the wall, where they are intercepted by different flow-stream velocities.

In TFFF, as in other FFF methods, each particulate or molecular species assumes a unique characteristic layer thickness within the channel as a function of the external force field and the channel characteristics. The highest population of sample components occurs near the wall, and this concentration continuously decreases with distance from the wall, following an exponential profile[7]

$$c(x) = c_0 e^{-x/l} \tag{1}$$

where x = the distance from the component-populated wall, $c(x)$ = the component concentration at distance x away from the wall, c_0 = the component concentration at the wall interface, and l = the characteristic component-layer thickness representing the center of gravity of the exponential profile. Since the concentration layer of smaller particles extends further toward the center of the channel where flow velocity is greater, small particles move faster, on average, than larger particles that are in slower flow streams nearer the wall.

The applied force field in FFF can be of any type that interacts with sample components and causes them to move perpendicular to the flow stream. The value of the mean particle-layer thickness l depends on the relative strength of the interaction between the applied external force and the opposing diffusion. Thus

$$l = D/U \tag{2}$$

where D = the particle–solvent diffusion coefficient (cm^2/s) and U = the velocity of the particle movement toward the wall (cm/s).[1] This relationship clearly establishes that l is the balance between two opposing influences; each

0024-9297/85/2218-2305$01.50/0

distinct particle identity has a unique l value depending on the different D/U values for the species.

Retention in FFF can be described by the dimensionless ratio λ[1]

$$\lambda = l/W = D/UW \tag{3}$$

where W is the thickness of the channel. The retention ratio R is defined as the ratio of the column void volume V_0 to the retention volume V_R of the eluted species. The retention ratio R is related to λ by

$$R = 6\lambda\ (\coth\ (1/2\lambda) - 2\lambda) \tag{4}$$

where coth $(1/2\lambda)$ = the hyperbolic cotangent of $(1/2\lambda)$. With highly retained peaks $R \simeq 6\lambda$ ($R < 0.3$ for component peaks eluting at least two channel volumes beyond the V_0 peak).

Retention in TFFF may be expressed as[7]

$$\lambda = \frac{1}{\left(\frac{a}{T} + \gamma\right)(\mathrm{d}T/\mathrm{d}x)W} \tag{5}$$

where the dimensionless thermal diffusion factor $a = (D_t T/D)$, D_t = the thermal diffusion coefficient, T = the temperature of the cold block (K), D = the solute diffusion coefficient, γ = the coefficient of thermal expansion of the solution, and $\mathrm{d}T/\mathrm{d}x$ = the temperature gradient in distance x. For homogeneous thermal field gradients $(\mathrm{d}T/\mathrm{d}x)W = \Delta T$. For small values of γ the following approximation can be made:

$$\lambda = \frac{1}{\left(\frac{a}{T}\right)\Delta T} = \frac{D}{D_t \Delta T} \tag{6}$$

In TFFF the mobile-phase velocity profile is not as well-defined as with the other FFF techniques, since mobile-phase viscosity varies with temperature across the channel width W.[7] This phenomenon disturbs the basic retention expressions somewhat because of a distortion of the normal parabolic flow profile.

As predicted by eq 6, larger temperature differences across the TFFF channel provide greater retention; therefore, high temperature differentials often are needed for retention of low molecular weight materials. As with the other FFF methods, in TFFF a very precise gap between highly polished flat plates is important to maintain maximum resolution. Field programming also can be used in TFFF, as in SFFF, to access a wide range of molecular weights in a single separation.[10] This is accomplished by gradually decreasing the ΔT between the two faces of the channel during the separation.

Experimental Section

Equipment. The TFFF instrumentation developed during this work provides flexibility in carrying out separations of polymeric materials. The equipment is arranged so that programming techniques can be used conveniently; samples with a wide molecular weight distribution can be readily characterized.

The arrangement of the TFFF equipment is shown schematically in Figure 1. Since various organic solvents are used as mobile phases in this technique, the unit is used in a hood to ensure good ventilation when solvent vapors may be present. A description of the components involved in this equipment follows.

An Isco Model 314 syringe-type displacement metering pump (Instrumentation Specialties Co., Lincoln, NE) generated the desired mobile-phase flow. This internal-reservoir pump delivers a pulseless flow and its well suited for the lower flow rates generally used in TFFF. The pump effluent is fed through a 0.5-μm porosity filter (Alltech Associates, Deerfield, IL). A Model C6W sample-loop injection valve (Valco Instruments, Houston, TX) is used to inject the sample into the channel.

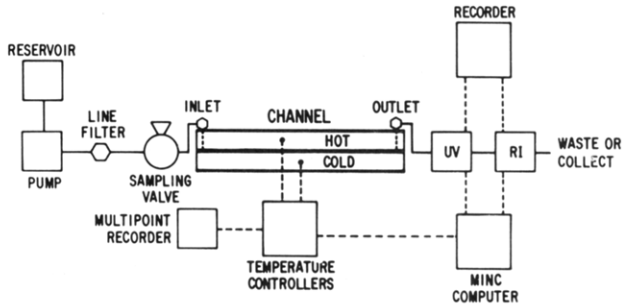

Figure 1. TFFF equipment schematic.

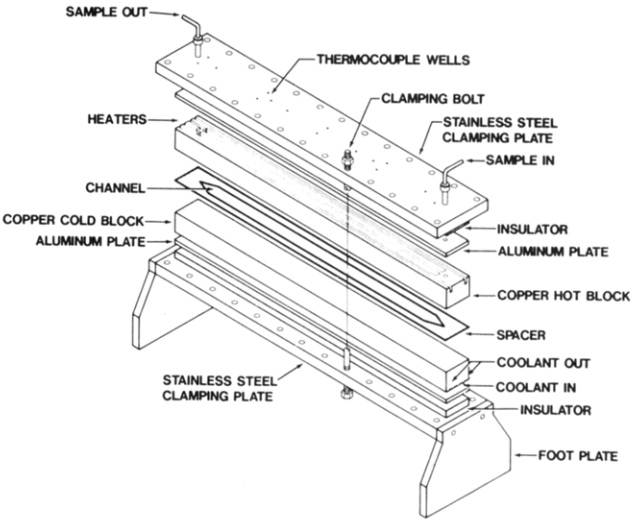

Figure 2. TFFF channel assembly, exploded view.

The TFFF separating channel is formed between two Ampcoloy-97 chromium–copper blocks (Ampo Metals, Inc., Milwaukee, WI), 61 cm long, 5.1 cm wide, and 3.8 cm thick. Compared to pure copper, this alloy exhibits superior machinability but still maintains 85% of the thermal conductivity. These copper blocks are separated by a 2.54-cm-wide channel spacer cut from Mylar polyester film (0.025 cm) or Kapton polyimide sheet (0.0076 or 0.0127 cm) (Du Pont). The channel was formed with a total length of 55.5 cm, with the ends shaped at 45° angles to produce a smooth-flowing inlet and outlet pattern.

The copper alloy blocks were machined to tolerances of ±50–75 μm across and down the channel face of the bar. They were then plated with 125–150 μm of chromium, and the plated sides of the bars were refinished. The flatnesses of each of the component faces of the finished channel were ±0.13 and ±0.21 μm, respectively. The surface finish of these chrome-plated faces were measured as approximately ±0.25 μm. Scratches remaining on the chrome-plated faces from the polishing process were generally <1.0 μm.

The bar/spacer assembly (Figure 2) was clamped together with 26 bolts ($^3/_8$ in. × 8 in., 16 threads/in.). Each bolt was fitted with several DD626 Belleville spring washers (Allied Devices Corp., Baldwin, NY) and then tightened to 15 ft-lb with a torque wrench. The end-view drawing in Figure 3 shows the resulting sandwich of a top (or bottom) stainless-steel plate, an insulating plate or epoxy-filled fiberglass, an aluminum retainer plate, and the copper bar, in that order. A retaining bar at the side of the channel assembly prevents possible extrusion of the spacer when pressuring the channel.

Ten narrow-gauge iron–constatan thermocouples were placed at 5-cm intervals along the top and bottom of each channel, about 1 cm from the edge, to monitor the temperature of the hot and cold plates over the entire surfaces. These thermocouples were inserted into wells drilled to within 75 μm from the interior face of the copper blocks. Thermocouples in the center of each block were used as sensing elements for the temperature controllers.

Samples were introduced into and subsequently eluted from inlet and outlet ports drilled through the hot (top) block, as shown

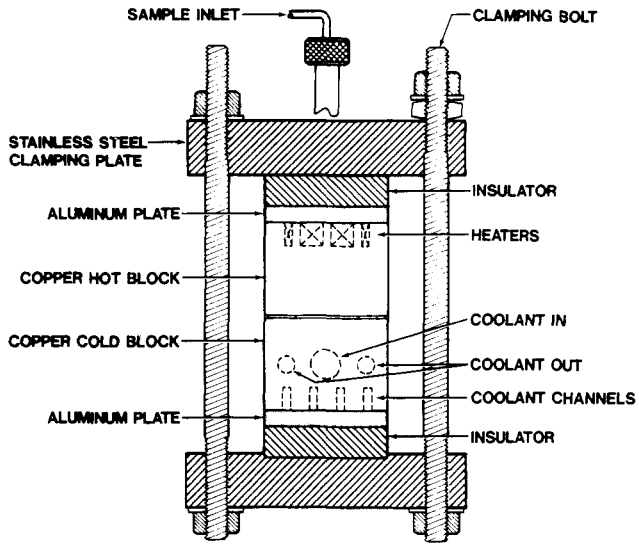

Figure 3. TFFF channel assembly, end view.

schematically in Figure 3. Heat was supplied to the hot copper block by two square contact resistance heaters and two smaller rectangular heaters totaling about 5 kW (at 240 V) (Figure 3). The temperature of the hot block was maintained at the desired level by an ECS Model 6416-5-X temperature controller (Electronic Control Systems, Fairmont, WV) with an ECS Model 7701-3-20-22 power module. An ECS Model 6250 oven-temperature controller was used as a safety device to ensure that the maximum temperature set for the system was not exceeded.

The temperature of the cold (bottom) block of the TFFF channel assembly was maintained by circulating a flow of cold 50% ethylene glycol–water mixture through channels cut in the bottom of the plate (see Figure 3). In this arrangement, flow from a circulating cooler entered the center two channels, proceeded to the end of the block, and then was led back through the outer two channels to the cold-bath reservoir. The temperature of the cold block was maintained with an ECS 6516-J-X temperature controller whose output actuated a Model 77-16 transducer (Moore Products Co., Spring House, PA), which in turn controlled two air-actuated controller valves (Badger Meter Co., Tulsa, OK). These proportioning valves controlled the amount of cold fluid available from a Model HX-300 Cool-Flo refrigerated circulator (Neslab Instruments, Portsmouth, NH), a 34 000-Btu water-cooled unit having a temperature range of −10 to +35 °C and a maximum pumped-liquid output of 24 L/min.

The output of the iron–constatan thermocouples inserted in the hot and cold blocks was continuously monitored with a Digistrip II digital multipoint recorder (Kaye Instruments, Bedford, MA). The set point of the temperature controllers for both the hot and cold blocks was established remotely with a MINC microcomputer (Digital Electronic Equipment, Maynard, MA). In-house software was developed to program the temperature of the hot and/or cold blocks during TFFF separations.

The effluent from the TFFF channel was passed through a Model 852 spectrophotometric detector (Du Pont Instruments, Wilmington, DE) via 0.5-mm i.d. connecting capillary tubing. In series with this spectrophotometric detector was an Optilab Model 5902 (interferometer) refractometer (Tecator Instruments, Herndon, VA). Output from these detectors was fed to a Model 7132A stripchart recorder (Hewlett Packard, Avondale, PA) and to the MINC computer, as illustrated in Figure 1.

Reagents. HPLC-grade solvents were used throughout the study. Polystyrene and poly(methyl methacrylate) molecular weight standards were obtained from Pressure Chemical Co. (Pittsburgh, PA) and Polymer Laboratories, Inc. (Amherst, MA), respectively. All other samples were secured within Du Pont.

Time-Delayed Exponential-Decay TFFF

Because of the high discrimination of TFFF to molecular weight differences, constant ΔT operation often produces inadequate resolution for components of lower molecular weight, while materials of higher molecular weight elute very late over very large increments of time. To overcome the limitations associated with constant-field (CF) TFFF temperature programming such as linear and parabolic systems have been used to decrease ΔT during the run.[10] Temperature programming speeds up the elution of higher molecular weight components, improves band spacing, reduces analysis time, and improves detection of later-eluting components. In this work, we have developed time-delay, exponential-decay TFFF programming (TDE-TFFF). This method has proved to be convenient for highly practical TFFF separations.

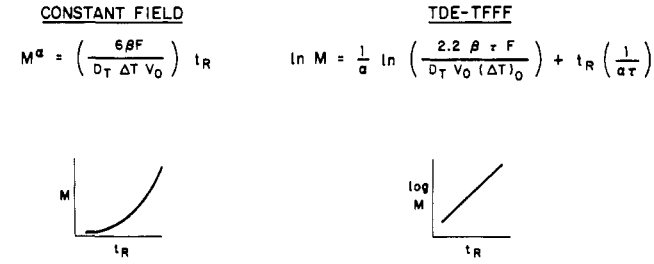

Figure 4. Molecular weight/retention time relationships in TFFF.

In CF-TFFF retention can be reasonably described by eq 6. It has been reported that the thermal diffusion coefficient D_t is not a function of molecular weight,[11,12] while the diffusion coefficient D is known to involve the relationship[13]

$$D = bM^{-\alpha} \tag{7}$$

where b = a constant, M = molecular weight, and α = 0.5–0.6 for random coil polymer conformations. Combining eq 6 and 7 leads to the expression

$$\lambda = \frac{bM^{-\alpha}}{D_t \Delta T} = \frac{\beta M^{-\alpha}}{\Delta T} \tag{8}$$

where $\beta = b/D_t$.

Since at significant retention $t_R = t_0/6\lambda$,[1] we find

$$t_R = \left(\frac{\Delta T M^\alpha}{6\beta}\right) t_0 \tag{9}$$

where t_R = retained component elution time and t_0 = elution time of an unretained component.

Therefore

$$M^\alpha = \left(\frac{6\beta}{\Delta T t_0}\right) t_R = \left(\frac{6\beta F}{V_0 \Delta T}\right) t_R \tag{10}$$

where F = mobile-phase flow rate (mL/min) and V_0 = channel dead volume.

Note that for CF-TFFF in eq 10 the retention time t_R is a fractional power function of molecular weight M. Thus, as illustrated in Figure 4, a plot of M vs. t_R in CF-TFFF produces an upward-curving relationship, indicating uneven resolution of components during a separation. The relatively large change in t_R with M in CF-TFFF also suggests difficulties in obtaining a separation of a wide range of molecular weights in a practical time span in this mode of operation because of the high discrimination of CF-TFFF between components with a relatively small MW difference. Further, the nonlinear M vs. t_R relationship in CF-TFFF produces data that are inconvenient for extracting quantitative molecular weight distributions. Finally, eq 10 predicts that retention time t_R is very much a function of flow rate F, ΔT, and the other operating parameters.

CF-TFFF limitations are largely overcome by the use of time-delayed exponential-decay temperature program-

ming (TDE-TFFF). This form of programming is analogous to time-delay exponential-decay programming used in SFFF.[14,15] In this experiment, the separation is initiated at $(\Delta T)_0$ for a time τ, and then ΔT is decreased exponentially, also with a time constant τ. Thus, $\Delta T = (\Delta T)_0$ for $t \leq \tau$, where τ is a time-delay constant; the temperature difference is then decreased exponentially by a decay-time constant that also equals τ; i.e., when $t > \tau$

$$\Delta T = (\Delta T)_0 e^{-(t-\tau)/\tau} \tag{11}$$

For highly retained components

$$L = \int_{t=0}^{t_R} (R v_0)\, dt = 6\beta v_0 M^{-\alpha} \int_{t=0}^{t_R} (1/\Delta T)\, dt \tag{12}$$

when

$$R = v_s/v_0 = t_0/t_R = \left(\frac{6\beta}{\Delta T}\right) M^{-\alpha} \tag{13}$$

with L = channel length (cm), t_0 = solvent peak-elution time, v_s = velocity of the solute migration down the channel (cm/s), and $v_0 = L/t_0$.

Equation 12 can be converted to

$$L = \left(\frac{6\beta v_0 M^{-\alpha} \tau}{e(\Delta T)_0}\right) e^{t_R/\tau} \tag{14}$$

and

$$M^{\alpha} = \left(\frac{6\beta v_0 \tau}{L e (\Delta T)_0}\right) e^{t_R/\tau} \tag{15}$$

or

$$\ln M = \left(\frac{1}{\alpha}\right) \ln \left(\frac{2.2\beta\tau F}{V_0 (\Delta T)_0}\right) + \frac{t_R}{\alpha\tau} \tag{16}$$

As illustrated in Figure 4, eq 16 predicts that in TDE-TFFF a plot of ln M (or $\log_{10} M$) vs. t_R should produce a straight-line relationship with a slope determined by the time-delay/decay constant τ and an intercept determined by the other operating parameters such as F and $(\Delta T)_0$. Equation 16 further suggests that TDE-TFFF operation should permit the analysis of a sample with a wide MW range in a relatively short time. Elution of sample components should be primarily controlled by τ, with less influence from F and other operating parameters compared to CF-TFFF.

TDE-TFFF experiments are performed in a very straightforward manner. The initial ΔT is established in a channel at a level required to separate the early-eluting components from the V_0 peak. The sample is injected with the mobile phase flowing at the flow rate needed for the analysis. This initial ΔT temperature is maintained for the time equivalent to τ, the delay/decay time constant, and then the ΔT is decreased exponentially, also with the time constant τ.

Results

Temperature Uniformity and Programming. Initial studies on the temperature homogeneity of the hot block of the TFFF channel indicated a significant falloff of temperature near the ends of the block. This apparently was due to two factors involved in the heater design. First, the resistance heater winding does not extend to the end of the heater shell. Second, there is an additional heat loss from the ends of the channel relative to the sides because of the higher surface area. To compensate for this temperature drop-off resistance heaters were used in which a higher wattage density was wound at the ends of the heater.

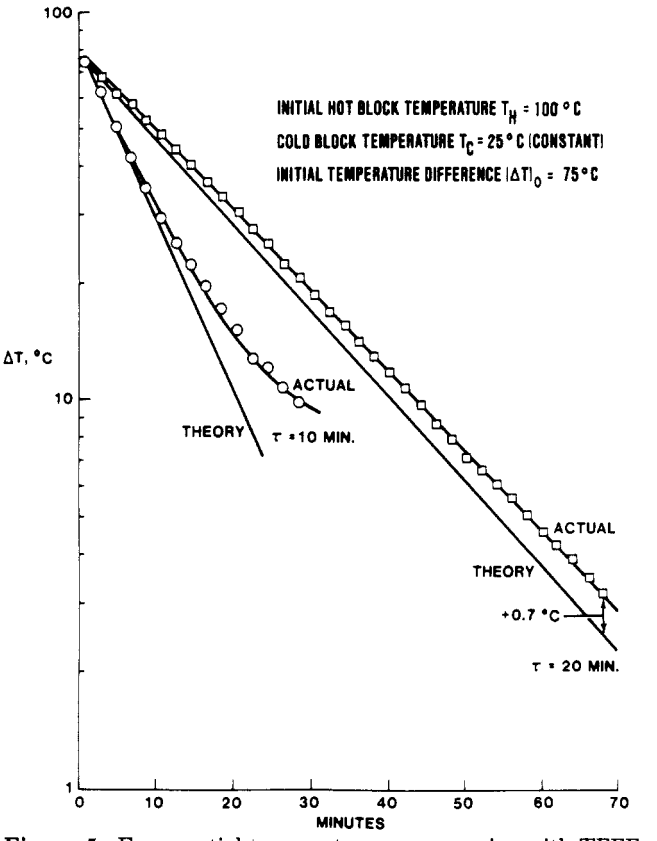

Figure 5. Exponential temperature programming with TFFF equipment.

Typically, temperature variation across the face of the channel was modest, usually $\leq \pm 0.5$ °C. Larger temperature variations were seen down the channel, and deviations of ±1.0 °C were typical for the hot block within ±15–18 cm from the center of the channel. Temperatures 4–5 °C below the hot-block set point have been observed in the vicinity of the inlet and the outlet because of difficulties in uniformly heating the block at the ends, even with specially wound heaters. Temperature uniformity of the cold block was much better; typically, variations down the channel were $\leq \pm 1\%$ and $\pm 0.1\%$ across the channel. This presumably is because of the better thermal transfer in the cold block by the relatively uniform flow of coolant throughout the "U"-shaped cooling channels and the high velocity of cooling fluid through the cold block.

The accuracy of the temperatures produced during time-delay/decay exponential programming is illustrated in Figure 5. The temperature measured at the center of the channels lags slightly behind the value set by the computer. Nevertheless, the measured log ΔT vs. time (min) relationship shows only a +0.7 °C error at the end of the programming run for τ = 20.0 min with an initial hot-block temperature of 100 °C and the cold-block temperature set at 25 °C.

Greater errors in ΔT values are observed with a τ = 10.0 min program (Figure 5) because of the inability of the hot block to cool fast enough to meet the programming goal. In our present apparatus the smallest delay/decay value that can be used with an initial hot-block temperature of 100 °C is about τ = 15.0 min. If the initial hot-block temperature is lower, smaller programming time constants can be used without significant errors.

During temperature programming at τ = 15 min, initial T_H = 93 °C, and final T_H and T_C = 15 °C, the variation

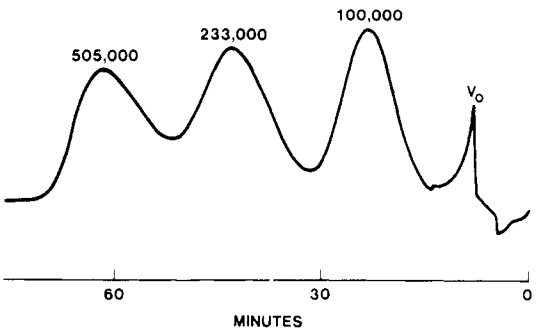

Figure 6. TFFF of narrow molecular weight polystyrene standards, constant temperature. Channel, 250 μm; mobile phase, dioxane; flow rate, 0.207 mL/min; hot-block temperature T_H, 100 °C; cold-block temperature T_C, 15 °C; detector UV, 254 nm; sample, 100 μL of 0.67 mg/mL each.

in the temperature along the length of the hot block (except at the extremes) was a maximum of about ±3 °C, with the central portion of the channel showing temperature variations of no more than ±2 °C maximum. Similarly, the cold block exhibited maximum temperature variations across the span of no more than ±1.3 °C, with a temperature variation along the length of no more than ±2–3 °C maximum (except at the very ends).

Applications

Polystyrenes. The resolving power of TFFF under constant ΔT conditions is illustrated in Figure 6 for the separation of narrow molecular weight polystyrene standards. Under the conditions for this separation (254-μm-thick channel) base-line separation was obtained with polystyrene standards with about a 2-fold difference in molecular weight. This level of resolution is roughly 5 times that which can be expected from high-performance size-exclusion chromatography (SEC). However, because of the large discrimination between molecular weights, the time required to elute components of higher molecular weight is relatively large in constant ΔT separations. Materials of very high molecular weight often require excessive time for elution under constant force-field conditions for a mixture where low MW components are well separated from V_0.

In contrast, in Figure 7 the TDE-TFFF separation of a series of polystyrene standards is carried out in about the same time as the CF-TFFF experiment in Figure 6, but with a much wider range of molecular weights eluted in a single experiment. This increase in the range of components in the same time span is accomplished by compromising the resolution between individual molecular weights of high MW species, a condition that is well justified in practical situations. Because of the large resolution of TDE-TFFF, instrumental band broadening in well-conducted experiments is small, and this effect causes no significant error on subsequent molecular weight measurements. No deconvolution of instrumental band broadening from total peak widths is needed for accurate quantitative measurements of molecular weight distribution.

The predicted linear log molecular weight vs. retention time relationship of eq 16 is verified by the data in Figure 8. A series of polystyrene standards shows a linear relationship with the anticipated exception at small retention times (near V_0). The theory of eq 16 further predicts that an increase in the delay/decay constant τ will decrease the slope of the calibration plot, with a small change of the intercept. This effect is confirmed in Figure 8 by the open points for τ = 15 and 30 min, respectively. Thus, an increase in the τ value provides greater resolution of components in the separation, but at a price of increased separation time.

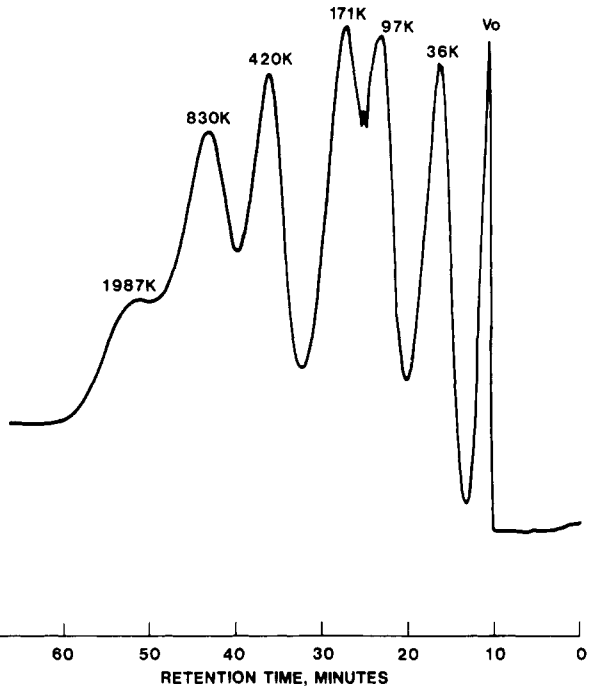

Figure 7. TDE-TFFF of narrow molecular weight polystyrene standards. Channel, 76 μm; mobile phase, dioxane; flow rate, 0.09 mL/min; initial hot-block temperature $(T_H)_0$, 70 °C; final hot-block temperature, 20 °C; cold-block temperature, 18 °C; τ delay/decay constant, 15.0 min; detector UV, 254 nm; sample, 25 μL of 0.83 mg/mL each.

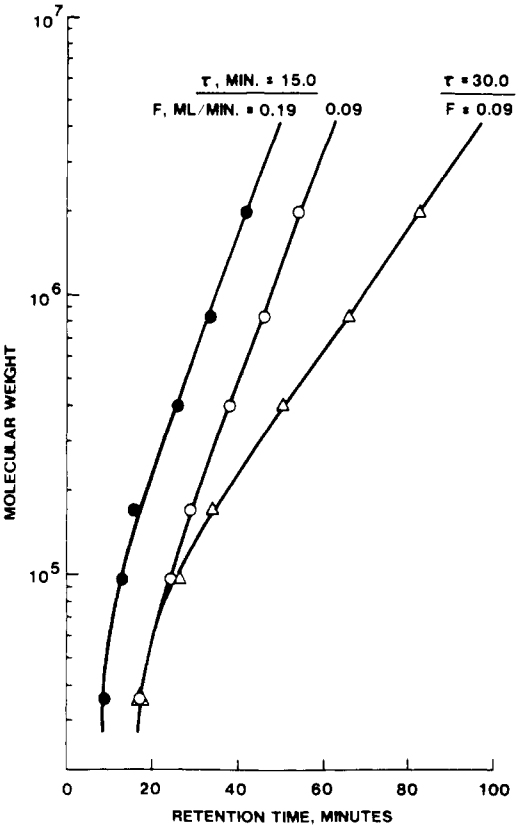

Figure 8. TDE-TFFF calibration with polystyrene standards. Conditions, same as for Figure 7 except flow rate and τ constant as shown.

The theory of eq 16 also predicts that changes in the other operating parameters for the TDE-TFFF separation (e.g., flow rate, channel thickness, etc.) will produce a

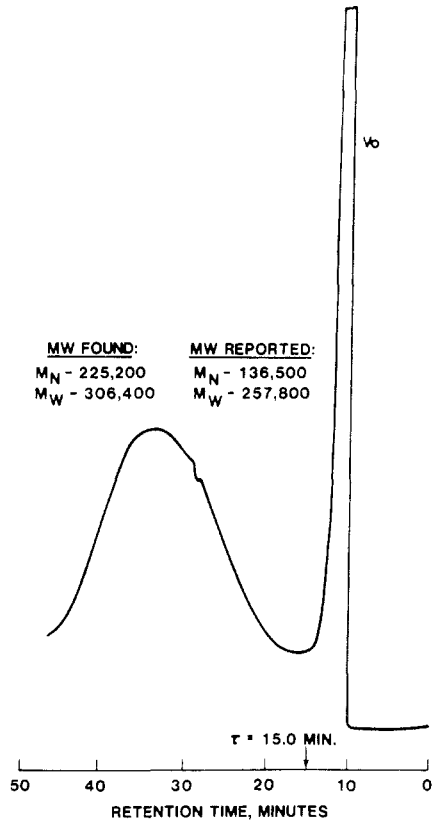

Figure 9. TDE-TFFF characterization of NBS 706 polystyrene broad molecular weight distribution standard. Conditions as in Figure 7.

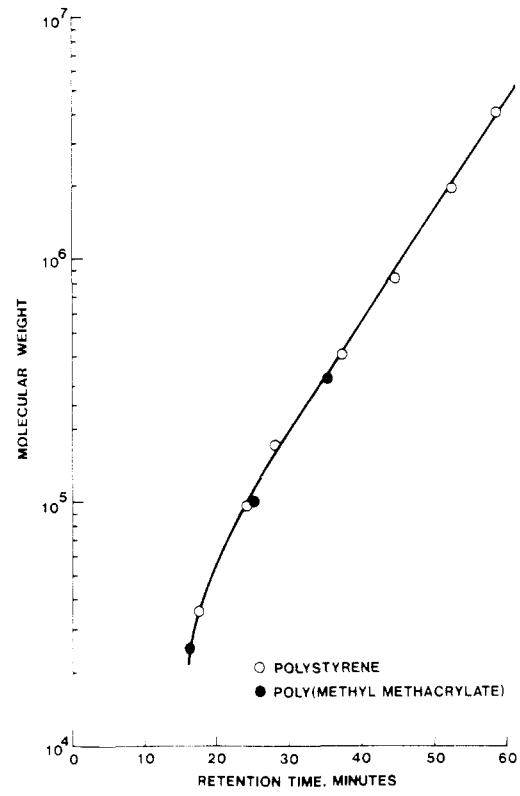

Figure 10. Molecular weight calibration curve for polystyrene and poly(methyl methacrylate) standards. Conditions as in Figure 7.

change in the intercept but not in the slope of the calibration plot. This effect also is demonstrated by the data in Figure 8 in which the flow rate was varied from 0.09 to 0.19 mL/min (constant τ = 15 min). Thus, a change in operating parameters other than τ will provide access to a different MW separating range, but with the same resolution.

Thus, in TDE-TFFF a variation in τ produces an effect comparable to changing column volume (e.g., column length) in SEC; the retention-time difference between peaks is altered, but the range of molecular weight separation remains the same. Variation in the other parameters (e.g., flow rate) is entirely analogous to changing pore size in SEC; molecular weight range accessed by the separation is altered, but resolution remains constant. Therefore, the effect of changing operating parameters in TDE-TFFF is essentially that in TDE-SFFF,[14,15] and the same general approaches for altering the conditions for the optimum separations can be used in both FFF methods.

Increasing the τ delay time tends to linearize the calibration plot for retention near V_0. Thus, more accurate data on peaks occurring close to the V_0 can be obtained by increasing the τ delay value to improve separation from V_0; the linearity of the calibration plot at small retention times also is improved.

The calibration data in Figure 8 and the theory of eq 16 predict that an increase in flow rate during a TDE-TFFF separation decreases retention time; however, the relative retention-time differences of individual components should not be significantly altered. This effect was observed in a separation which was identical to that in Figure 8 except that the flow rate was doubled. As predicted, all of the peaks were shifted toward V_0, retention-time difference between the peaks was essentially unchanged, and the time required for the separation was somewhat decreased. However, resolution of the component of lowest molecular weight (36 000) from the V_0 peak was degraded. Thus, the various operating parameters of TDE-TFFF can be easily and conveniently altered to produce the resolution and separating range required for a particular separation.

The availability of the polystyrene peak position calibration plot in Figure 8 permits the analysis of broad MW polystyrene samples such as that shown in Figure 9. The calculated molecular weight values for the NBS 706 broad polystyrene standard correspond fairly well with those reported for this sample. It should be noted that the absolute accuracy of this particular TDE-TFFF analysis is somewhat complicated by the fact that dioxane showed an unexpected base-line drift near V_0 during the run, making a number-average calculation somewhat imprecise. This artifact related specifically to the particular experiment using dioxane and is not an inherent function of TDE-TFFF separations.

Characterization of Poly(methyl methacrylate). The thermal diffusion factor for PMMA in dioxane apparently is very similar to that of polystyrene, resulting in very similar retentions. Figure 10 shows that three secondary PMMA standards produced TFFF data corresponding closely to that of polystyrene standards. This fortunate circumstance suggests that the polystyrene calibration curve in Figure 10 would provide a reasonable means of estimating the molecular weight of appropriate high MW PMMA samples, even though high MW PMMA standards were not available. The calibration curve of Figure 10 also suggests that the total range of usable calibration for these particular operating conditions is >4 × 10^6 MW, although this does not represent the upper molecular-weight-range capability of TFFF with other operating conditions. While SEC often is unable to produce reliable measurements with polymers above about 10^6 MW, the open-channel TFFF method can separate very high molecular weight materials with none of the

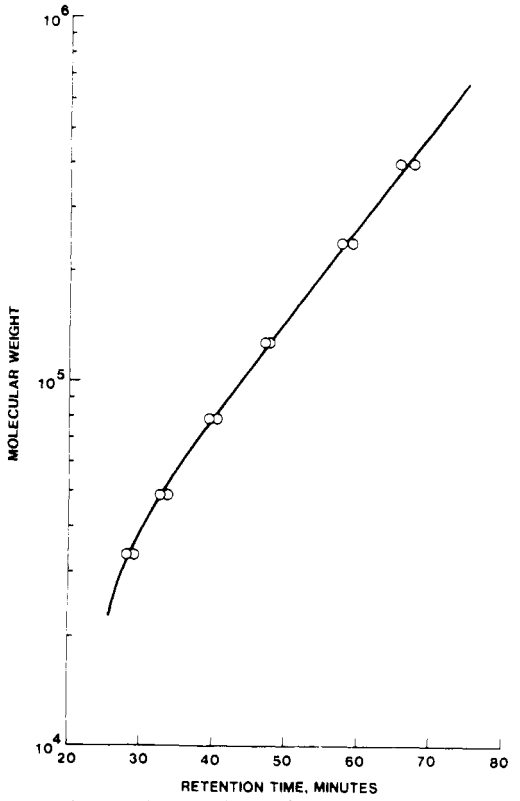

Figure 11. Molecular weight calibration curve for poly(methyl methacrylate). Channel, 125 μm; mobile phase, dioxane; flow rate, 0.15 mL/min; initial hot-block temperature, 100 °C; final hot-block temperature, 20 °C; cold-block temperature, 20 °C; τ delay/decay constant, 20.0 min; detector RI, X250; sample, 100 μL, 1 mg/mL in dioxane.

difficulties associated with packed-bed methods. Not only are high MW polymers sometimes eluted with difficulty from SEC systems, but problems with the shear degradation of high MW polymers also have already been noted in SEC studies.[16]

The TDE-TFFF calibration plot for a series of narrow molecular weight PMMA standards is shown in Figure 11. Again, as predicted by eq 16, the log MW vs. retention time plot in this τ = 20.0 min program is linear (except near V_0). Duplicate calibration points for each PMMA standard were obtained during a 3-day period, illustrating the level of reproducibility of obtaining TDE-TFFF data with the present apparatus.

Molecular weight distribution (MWD) determinations were carried out for broad MWD PMMA samples by using the peak-position calibration plot in Figure 11. Figure 12 shows the fractogram for Lucite 40 acrylic resin, a broad MWD PMMA secondary standard used in SEC characterization. The weight-average, M_w, and number-average molecular weight, M_n, as well as polydispersity (M_w/M_n), agree well for the two methods. However, the method used for TFFF calibration by peak position using narrow MWD standards together with supplementary SEC and quasi-elastic light-scattering studies suggest that the TDE-TFFF values actually are more accurate.

Data from the refractive (RI) index detector in Figure 12 produced results that were more easily interpreted, relative to UV detection at 215 nm, because of reduced

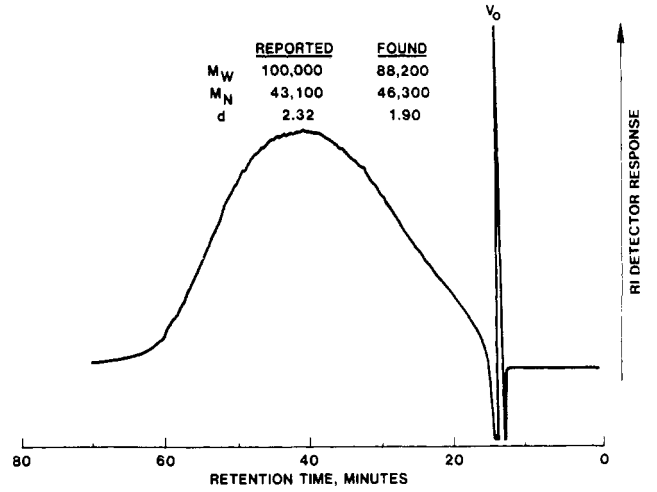

Figure 12. Molecular weight characterization of Lucite 40 acrylic resin by TDE-TFFF. Conditions as in Figure 11.

interference by the overlapping V_0 peak with the particular separation conditions used. These and other results suggest that the interferometer RI detector may be superior in applications involving compounds that must be detected at lower UV wavelengths. The adsorption index of C=O absorption at 215 nm for PMMA is relatively small, and in such situations RI detection by the highly sensitive interferometer RI may be preferred.

Acknowledgment. Special thanks are given to C. H. Dilks, Jr., for assisting in the design and construction of the TFFF equipment and for performing many of the experiments, and to J. C. Fogg and D. R. Petrak, who also assisted in design and fabrication. We also acknowledge the important contribution of D. W. St. Clair in designing the temperature control system.

Registry No. Polystyrene (homopolymer), 9003-53-6; Lucite 40, 87003-70-1.

References and Notes

(1) Giddings, J. C.; Fisher, S. R.; Myers, M. N. *Am. Lab. (Fairfield, Conn.)* **1978**, *10*, 15.
(2) Giddings, J. C.; Myers, M. N.; Caldwell, K. D.; Fisher, S. R. *Methods Biochem. Anal.* **1980**, *26*, 79.
(3) Kirkland, J. J.; Rementer, S. W.; Yau, W. W. *Anal. Chem.* **1981**, *53*, 1730.
(4) Kirkland, J. J.; Dilks, C. H., Jr.; Yau, W. W. *J. Chromatogr.* **1983**, *255*, 255.
(5) Thompson, G. H.; Myers, M. N.; Giddings, J. C. *Anal. Chem.* **1969**, *41*, 1219.
(6) Hovingh, M. E.; Thompson, G. H.; Giddings, J. C. *Anal. Chem.* **1970**, *42*, 195.
(7) Myers, M. N.; Caldwell, K. D.; Giddings, J. C. *Sep. Sci.* **1974**, *9*, 47.
(8) Giddings, J. C.; Martin, M.; Myers, M. N. *J. Chromatog.* **1978**, *158*, 419.
(9) Grew, J. C. "Transport Phenomena in Fluids"; Hanley, H. J. M., Ed.; Dekker: New York, 1969; Chapter 10.
(10) Giddings, J. C.; Smith, L. K.; Myers, M. N. *Anal. Chem.* **1976**, *48*, 1587.
(11) Norberg, P. H.; Claesson, S. *Acta* IMEKO **1964**, *4*, 501.
(12) Meyerhoff, G.; Lütje, J.; Ranch, B. *Makromol. Chem.* **1961**, *44–46*, 489.
(13) Flory, P. J. "Principles of Polymer Chemistry"; Cornell University Press: Ithaca, NY, 1953.
(14) Yau, W. W.; Kirkland, J. J. *Sep. Sci. Technol.* **1981**, *16*, 577.
(15) Kirkland, J. J.; Yau, W. W. U.S. Patent 4 285 810, Aug 25, 1981.
(16) Kirkland, J. J. *J. Chromatogr.* **1976**, *125*, 231.